

# Hardware Design for Compact and Accurate Wearable Cutaneous Haptic Device in Avatar Systems

Hyunsu Kim, Harim Ji, Somang Lee and Dongjun Lee

**Abstract**—We present the development of a wearable Cutaneous Haptic Device (CHD) for avatar systems, focusing on improvements in force sensing and hardware architecture. The contact of the Force-Sensitive Resistor (FSR) sensor is located to feature a larger prime sensing zone, enhancing measurement accuracy across different configurations of the CHD. This allows for more reliable force feedback, improving system responsiveness and user interaction. The CHD hardware is optimized by transitioning to a PCB-based architecture, reducing wiring complexity, increasing durability, and enhancing user comfort.

## I. INTRODUCTION

As robots increasingly integrate into our daily lives, they must be capable of performing dexterous manipulation tasks, which are often complex and require an understanding of interactive forces [1]. Humans, the leader of avatar systems, use the fingertips to maintain grasp stability by applying forces normal to the object surface to counter-act tangential forces that arise due to slip, rotation of the object, and its weight [2]. In many scenarios of the avatar system, robotic hands can be equipped with sensors that provide fingertip force information using tactile or force/torque sensor [3]-[6], which is then delivered to the operator. Thus, the precise haptic feedback allows the operator to perform delicate tasks with confidence and high accuracy.

To provide fingertip force information, Cutaneous Haptic Devices (CHDs) have been developed with a focus on miniaturization [7]-[9] to ensure practical use. Lee et al. [10] design the CHD to be worn on the fingertip and operated in three degrees of freedom. The design of such CHDs is critical as the device must be small and robust, as hardware improvements directly lead to control performance. In this study, we enhance the CHD developed in [10], by integrating a Force Sensitive Resistor (FSR) sensor with a larger prime sensing zone and transiting to a PCB-based architecture, which reduces wiring complexity, minimizes weight, and improves durability. The effectiveness of these improvements is demonstrated through control performance evaluation.

## II. PRELIMINARY

Due to the small size of CHDs, precise control requires accurate modeling. For kinematic modeling, the system is designed with a symmetric base part and a contact part as

\*This work was supported by the National Research Foundation of Korea (NRF) Grant funded by the Korean Government (MSIT) (RS-2023-00208052).

The authors are with the Department of Mechanical Engineering and IAMD, Seoul National University, Seoul, Republic of Korea, 08826. {hyunsu.kim, jiharim0911, hopelee, djlee}@snu.ac.kr. Corresponding author: Dongjun Lee.

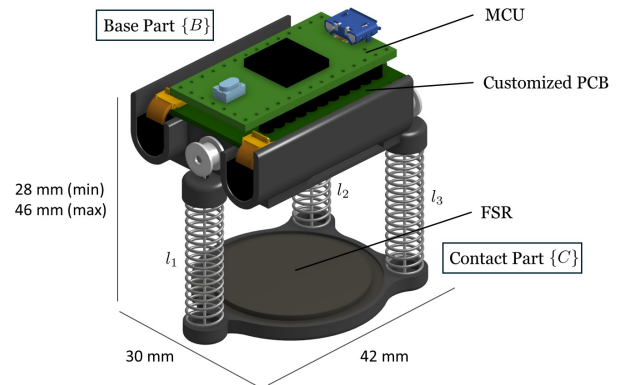


Fig. 1. Hardware architecture of the wearable CHD

shown in Figure 1. Their relative rotation is fully described in terms of the tendon lengths  $l \in \mathbb{R}^3$ . Thus,  $l$  can be decomposed into a configuration-defining state  $q$  and its counterpart  $\xi$ .

$$l = J^\dagger q + N_J \xi \quad (1)$$

where  $J \in \mathbb{R}^{2 \times 3}$  is a constant Jacobian defined by the position of the tendon depending on the base part and contact part,  $J^\dagger := J^T (JJ^T)^{-1} \in \mathbb{R}^{3 \times 2}$ , and  $N_J \in \mathbb{R}^{3 \times 1}$  is the kernel of  $J$ .

The contact force generated by the motor output and the compressed spring force act perpendicularly to the virtual plane  $\{M\}$  as shown in Figure 2. The contact force,  $f$ , measured in the FSR is as follows:

$$\begin{aligned} f e_{3,B}^T e_{3,M} &= K(q)(l - l_0) + u \\ &= K(q) [J^\dagger (q - q_0) + N_J (\xi - \xi_0)] + u \end{aligned} \quad (2)$$

where  $e_{3,B}$  and  $e_{3,M}$  is unit vector perpendicular to plane  $\{B\}$  and  $\{M\}$  respectively,  $K(q)$  is stiffness matrix of springs, and  $u$  is control input by motors.

## III. HARDWARE ENHANCEMENT

### A. Force sensing using FSR

In [10], the contact part is divided into two parts: the upper part, which the finger touches, and the lower part, where the tendon is connected. The FSR sensor is placed between these two parts to measure contact force. This is because the FSR sensor can only accurately measure within a small effective range, roughly 5.6 mm in diameter. When the haptic input is zero, the FSR sensor should not be in contact, enforcing small springs to be inserted between the upper and lower parts. These springs mediate relative rotation between the

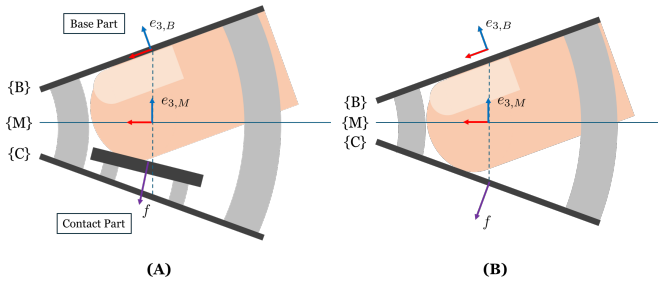


Fig. 2. Schematic diagram of the (A) previous and (B) current CHD when the fingertip is in contact

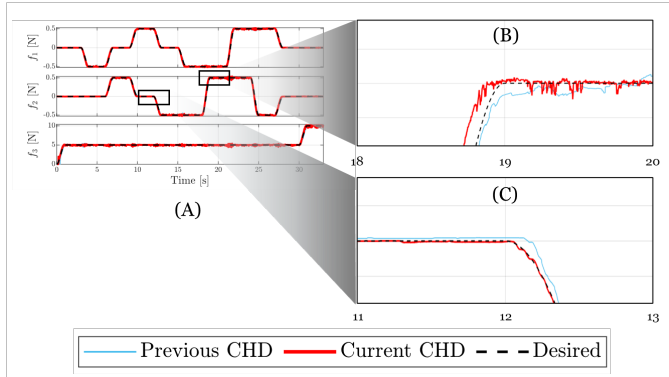


Fig. 3. Comparison of contact force trajectory tracking performance for the previous and current CHD (A) overall (B) response to a rising step (C) response to a falling step

two parts, making it challenging to accurately project the FSR sensor values to plane  $\{M\}$ .

We adopt an FSR sensor (RA30P, MarvelDex) with a larger prime sensing zone ( $\phi = 24$  mm), capable of accurate measurement for all contact in configurations of the CHD. In [10], the controller implicitly regulates the spring-induced dynamics, but with the spring structure removed, we improve precision as shown in Table I. The removal of the spring structure is possible because the fingertip itself has sufficient deformation capability, allowing it to naturally deform in the direction of the force that acts perpendicular to the virtual plane  $\{M\}$ . The removal of the spring structure also leads to improvements in durability, weight reduction, and enhanced stability during wear.

### B. PCB-integrated modules

To minimize the load applied directly to the user's fingertip, the previous CHD hardware design separates the components into a control module and an actuation & sensing module. The control module, which consists of a motor driver and a microcontroller (Teensy 4.0, PJRC), is attached to the forearm or laid on the table, and the actuation & sensing module contains the motors, encoders and an FSR sensor along with a converter. In order to improve compactness, the control module is integrated into a custom PCB, designed as a shield for the microcontroller. As a result, all the hardware necessary for CHD operation is integrated onto the fingers, significantly reducing the overall weight (from 30g (Main device) + 70g (The control modules) to 35g (Device-

TABLE I  
CONTROL PERFORMANCE EVALUATION

		Contact Force		
		$f_1$	$f_2$	$f_3$
Previous	RMSE [N]	0.0098	0.0102	0.1642
	NRMSE [%]	0.9758	1.0244	1.6419
Current	RMSE [N]	0.0056	0.0063	0.0872
	NRMSE [%]	0.5555	0.6345	0.8724

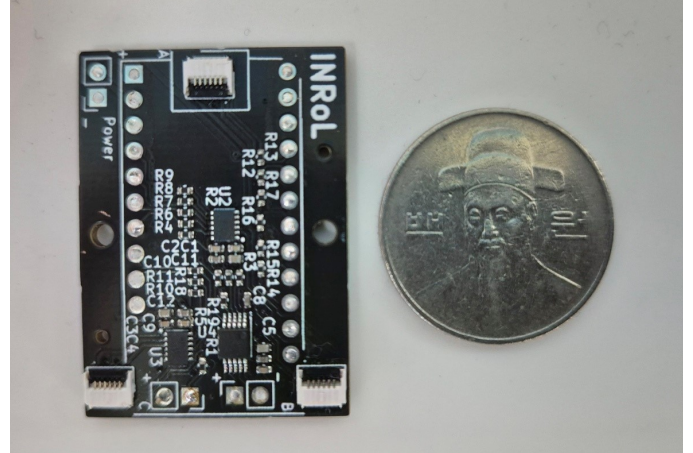


Fig. 4. Comparison of the size between the customized PCB and a coin ( $\phi = 24$  mm)

wide)). This also resolves movement restrictions caused by the modular connections and cable stiffness, making it more practical for real-world applications.

## IV. CONCLUSIONS

We introduce modifications in the FSR sensor and PCB-integrated modules to enhance precision and performance in the previous CHD. We apply a sensor featuring a larger prime sensing zone, enabling the elimination of spring elements. We also transit the system's components to a PCB-based architecture. The resulting system shows improved performance still enhancing usability. For future work, we plan to conduct user studies focused on haptic feedback to evaluate the effectiveness of the system in delivering precise tactile sensations during teleoperation tasks.

## REFERENCES

- [1] Billard, Aude, and Danica Kragic. "Trends and challenges in robot manipulation." *Science* 364.6446 (2019): eaat8414.
- [2] Johansson, Roland S., and J. Randall Flanagan. "Coding and use of tactile signals from the fingertips in object manipulation tasks." *Nature Reviews Neuroscience* 10.5 (2009): 345-359.
- [3] Kim, Kyungsoo, et al. "Tactile avatar: Tactile sensing system mimicking human tactile cognition." *Advanced Science* 8.7 (2021): 2002362.
- [4] Sarakoglou, Ioannis, et al. "A high performance tactile feedback display and its integration in teleoperation." *IEEE Transactions on Haptics* 5.3 (2012): 252-263.
- [5] Su, Hang, et al. "Deep neural network approach in robot tool dynamics identification for bilateral teleoperation." *IEEE Robotics and Automation Letters* 5.2 (2020): 2943-2949.
- [6] Patel, Rajni V., S. Farokh Atashzar, and Mahdi Tavakoli. "Haptic feedback and force-based teleoperation in surgical robotics." *Proceedings of the IEEE* 110.7 (2022): 1012-1027.
- [7] Giraud, Frederic H., Sagar Joshi, and Jamie Paik. "Haptigami: A fingertip haptic interface with vibrotactile and 3-DoF cutaneous force feedback." *IEEE Transactions on Haptics* 15.1 (2021): 131-141.

- [8] Prattichizzo, Domenico, et al. "Towards wearability in fingertip haptics: a 3-dof wearable device for cutaneous force feedback." *IEEE Transactions on Haptics* 6.4 (2013): 506-516.
- [9] Lee, Yongjun, et al. "Wearable finger tracking and cutaneous haptic interface with soft sensors for multi-fingered virtual manipulation." *IEEE/Asme Transactions on Mechatronics* 24.1 (2018): 67-77.
- [10] Lee, Somang, Hyunsu Kim, and Dongjun Lee. "Symmetry-Based Modeling and Hybrid Orientation-Force Control of Wearable Cutaneous Haptic Device." *2023 IEEE/RSJ International Conference on Intelligent Robots and Systems (IROS)*. IEEE, 2023.